

# The influence of rotation on the $\beta_N$ threshold for the 2/1 neoclassical tearing mode in DIII-D<sup>a)</sup>

R. J. Buttery,<sup>1,b)</sup> R. J. La Haye,<sup>2</sup> P. Gohil,<sup>2</sup> G. L. Jackson,<sup>2</sup> H. Reimerdes,<sup>3</sup> E. J. Strait,<sup>2</sup>  
and the DIII-D Team

<sup>1</sup>EURATOM/UKAEA Fusion Association, Culham Science Centre, Abingdon,  
Oxfordshire, OX14 3DB, United Kingdom

<sup>2</sup>General Atomics, P.O. Box 85608, San Diego, California 92186-5608, USA

<sup>3</sup>Columbia University, New York, New York 10027, USA

(Received 14 November 2007; accepted 18 February 2008; published online 15 April 2008)

Utilizing a capability to vary neutral beam torque injection in the DIII-D [J. L. Luxon, Nucl. Fusion **42**, 614 (2002)] tokamak,  $m/n=2/1$  neoclassical tearing mode onset thresholds are found to fall by about one unit in  $\beta_N$ , from  $\sim 3$  to  $\sim 2$ , in ITER-like sawtoothed high-energy confinement modes of plasma operation [R. Aymar, Plasma Phys. Control. Fusion **42**, B385 (2000)] as “co-injected” torque and rotation are reduced. However, increasing levels of torque and rotation in the counter-direction do not lead to corresponding rises in  $\beta_N$  thresholds. More encouragingly, error field sensitivity is not found to increase in low rotation plasmas, as might be expected theoretically. These results pose an interesting physics problem, as well as raising concern for future devices such as ITER. Further analyses have explored possible physics origins of the behavior. They suggest many of the usual effects expected to lead to a rotation dependence (mode coupling, wall drag, ion polarization currents) are not significant, with instead models that depend on the size and sign of rotation shear playing a role. Onset behavior suggests the mode is close to being intrinsically (classically) unstable when it appears, and a conceptual explanation is offered for a mechanism by which rotation shear feeds into the onset process through changes to the classical tearing stability index,  $\Delta'$ . Further parameter extensions and studies are desirable to fully resolve the underlying physics of this interesting process. [DOI: 10.1063/1.2894215]

## I. INTRODUCTION

A key issue for ITER is the extrapolation of the onset threshold and control requirements for the neoclassical tearing mode (NTM), expected to account for the principal performance limit of both the ITER baseline and hybrid scenarios.<sup>1</sup> However, the behavior of this instability remains challenging to understand, with many uncertainties in the theory, both to understand which models will dominate and to quantify the models. These difficulties are exacerbated in the prediction of ITER, which requires extrapolation in two key variables— $\rho^*$  and rotation (where here  $\rho^*$  is ion poloidal Larmor radius normalized to resonant surface minor radius)—that are fundamental to the behavior of much of the underlying physics. Of concern is that ITER is unlikely to benefit from the stabilizing influence of the high plasma rotation driven by strong neutral beam momentum injection in most present devices. It will also operate at low  $\rho^*$ , where small island stabilization effects will be reduced, making NTM triggering easier.

The main elements of uncertainty in ITER prediction come both from the initial island triggering process (the “seeding”) and the NTM threshold physics. For example, if the seeding is due to magnetic coupling,<sup>2,3</sup> then differential rotation between resonant surfaces would play a strong role

in influencing NTM  $\beta$  thresholds (where  $\beta$  is the ratio of thermal energy relative to magnetic energy in the plasma). But if islands are formed due to a  $\beta$  related pole<sup>4,5</sup> in the classical tearing stability index,  $\Delta'$ , then threshold variations may be weaker. Variations in the underlying NTM drives can also contribute. For example, the commonly observed  $\rho^*$  scaling of NTM  $\beta$  thresholds<sup>3,6–8</sup> arises from the small island size stabilization mechanisms.<sup>9–11</sup> But if these small island terms are dominated by ion polarization current effects, then a strong dependence is also expected on island rotation in the zero perpendicular electric field frame of reference.<sup>12</sup>

In this paper we explore these issues for the most serious of these modes, the 2/1 NTM (denoting *poloidal/toroidal* mode numbers), which if unchecked, is found to approximately halve the plasma energy confinement and can also trigger plasma terminations.<sup>13</sup> We start by summarizing the origins of rotation dependence in Sec. II—exploring both the underlying theory and previous experimental work. In Sec. III we describe the experiment design and show a typical discharge. Then in Sec. IV we detail the rotation dependencies identified in the experiments, summarizing the main trends and exploring more subtle parameter dependencies to gain insight into the processes involved. These results are then discussed in the context of the triggering physics and a possible model that can explain the observed trends in Sec. V, with the implications for scaling considered. We present our conclusions in Sec. VI.

<sup>a)</sup>Paper U11 3, Bull. Am. Phys. Soc. **52**, 313 (2007).

<sup>b)</sup>Invited speaker. Electronic mail: richard.buttery@ukaea.org.uk.

## II. ROLE OF ROTATION IN NTM PHYSICS

To understand how the various physical mechanisms combine to trigger a NTM, it is useful to consider the modified Rutherford equation,<sup>14,15</sup> which governs the evolution of an island of full width,  $w$  and minor radius,  $r$ ,

$$\frac{\tau_r dw}{r dt} = r(\Delta'_o - \alpha w) + r\beta_p \times \left[ a_{bs} \left( \frac{0.65w}{w^2 + w_d^2} + \frac{0.35w}{w^2 + 28w_b^2} \right) - \frac{a_{GGJ}}{\sqrt{w^2 + 0.2w_d^2}} - \frac{a_{pol}w}{w^4 + w_b^4} \right]. \quad (1)$$

Here the NTM is driven by a helical hole in the bootstrap current<sup>16</sup> that develops about an island due to pressure flattening (the  $a_{bs}$  or “bootstrap” term); this is dependent on the local poloidal  $\beta$ ,  $\beta_p$  (with a small correction for field curvature,<sup>17</sup> the  $a_{GGJ}$  term). Once triggered, islands rapidly grow (on a resistive time scale,  $\tau_r$ ) to a saturated size which to first order depends on the ratio of the bootstrap term to the classical tearing stability index [the  $r(\Delta'_o - \alpha w)$  term, where the  $\alpha$  introduces an island size dependence that accounts for saturation of tearing modes<sup>18</sup>].

With just the above discussed terms, NTMs would grow from zero island width in all discharges with positive shear at a rational  $q$  (the safety factor) flux surface. However, the  $w_d$ ,  $a_{pol}$ , and  $w_b$  terms act to make the NTM stable at small island size (and low  $\beta$ ) leading to the need for a seeding event, required to induce a large enough island for bootstrap driven growth to take over. These small island terms are due, respectively, to the effects of ion polarization currents<sup>9</sup> ( $a_{pol}$  term), finite transport over the island<sup>10</sup> ( $w_d$  term), and the loss of bootstrap as island size approaches ion banana widths<sup>11</sup> ( $w_b$  term). They lead to a  $\beta$  threshold for metastability of the mode, below which the NTM is unconditionally stable. These terms play a crucial role in introducing rotation and  $\rho^*$  dependencies, both directly in the parameters that govern these small island effects, and through the requirement for a seeding event, which may also depend on these parameters.

As an example, ion polarization current effects can be characterized by<sup>12</sup>

$$a_{pol} \propto g(\nu, \varepsilon) (L_q/L_p)^2 \rho_{i\theta}^2 \Omega (\Omega - \omega_i^*) / \omega_e^{*2}, \quad (2)$$

where “ $g$ ” is a function of normalized collisionality,  $\nu = \nu_i / \varepsilon \omega_e^*$ , with  $g=1$  for  $\nu \ll 1$ , and  $g = \varepsilon^{-3/2}$  for  $\nu \gg 1$ ;  $\nu_i$  is the ion collision frequency,  $\omega_e^*$  ( $\omega_i^*$ ) is the electron (ion) diamagnetic frequency, and  $\rho_{i\theta}$  is the poloidal ion Larmor radius (all quantities taken at the relevant resonant surface). This term also depends on the natural island propagation frequency in the zero radial electric field frame of reference ( $\Omega = \Omega_{NTM} - \Omega_{E_\perp=0}$ ). Assuming the  $\Omega$  term is constant and leads to a positive (stabilizing) sign for  $a_{pol}$ , then folding Eq. (2) back into Eq. (1), neglecting  $w_d$  and  $w_b$  terms, and assuming a given “seed” island size,  $w = w_{seed}$ , we can solve for

marginal growth ( $dw/dt=0$ ) to give a threshold for NTM onset in  $\beta_p$ ,  $\beta_{p-onset}$ , which scales with  $\rho^*$ ,

$$\sqrt{\frac{L_q}{L_p}} \beta_{p-onset} \propto -r_s \Delta' \rho_{i\theta}^* \frac{w_{seed}/w_{pol}}{[1 - (w_{pol}/w_{seed})^2]} g(\nu, \varepsilon), \quad (3)$$

where  $w_{pol}^2 = a_{pol} / (a_{bs} \varepsilon^{1/2} L_q / L_p)$  and  $\rho_{i\theta}^* = \rho_{i\theta} / r_s$ .

A key element this establishes is the link between the  $\beta_{p-onset}$ , and the seed island size at NTM onset. When  $w_{seed}$  is small, very high  $\beta_p$  is required for neoclassical growth, but as seed size increases the  $\beta_{p-onset}$  falls, reaching a minimum at  $w_{seed} = \sqrt{3} w_{pol}$ . A similar form can be obtained with the finite island transport model ( $w_d$ ), as discussed in Refs. 3, 7, 10, and 19.

In some situations the distinction between the seeding and the NTM evolution can also become mixed, for example, where high  $\beta_N$  leads to a rise in  $\Delta'$  associated with a  $\Delta'$  pole at high  $\beta_N$ ,<sup>5</sup> initiating *classical* island growth that is then driven further by the bootstrap term.<sup>4,20</sup> In these cases, the small island terms will still be important in setting the degree to which  $\beta_N$  must rise in order to make  $\Delta'$  sufficiently large to overcome the small island terms and drive island size to the point where neoclassical effects (the loss of bootstrap due to pressure flattening) can amplify island size further. (Here  $\beta_N$  is defined as the ratio of  $\beta$  to the quantity  $I_p / aB_T$ , where  $I_p$  is plasma current,  $a$  is the minor radius, and  $B_T$  is toroidal field). This point may be particularly significant where external seeding processes [e.g., an island being driven by other magnetohydrodynamic (MHD) events] may be weak, such as in hybrid scenarios for the 2/1 NTM, where strong sawtooth activity is avoided.

Considering the above formalism we see various mechanisms by which rotation can influence behavior:

1. First, the dependence enters through the ion polarization current term. This can have a strong effect, flipping the sign of the term to either drive or suppress tearing. But the significance of this effect also depends on how much ion polarization current mechanisms dominate over other small island size effects.
2. If the NTM is triggered by magnetic coupling to some secondary event [e.g., toroidal<sup>2</sup> or three wave<sup>21</sup> coupling to core instabilities, or possibly to edge localized modes (ELMs)], then the perturbation at the NTM resonant surface will be shielded out by differential rotation with respect to the applied perturbation (e.g., a sawtooth precursor). In addition, the triggering instability itself may have a dependence on rotation, as is observed for the sawtooth instability.<sup>22,23</sup>
3. Changes in rotation can influence the  $\Delta'$  directly due to changes in interaction between resonant surfaces<sup>24</sup> and through rotation shear at the NTM resonant surface.<sup>25,26</sup> These effects can depend on the sign of rotation shear with respect to that of magnetic shear, although the physics is complex and can depend on further derivatives.
4. The interaction of a rotating mode (particular if near the plasma edge, such as the 2/1 NTM) with the vessel wall may have a stabilizing effect on the mode.

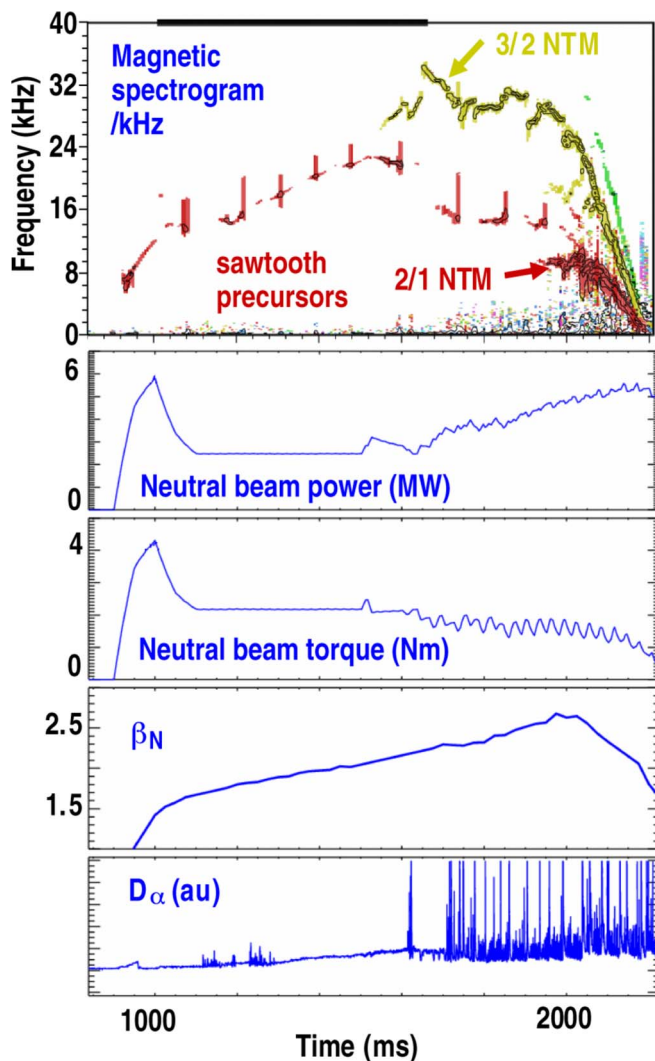


FIG. 1. (Color online) Typical shot time history (shot number 126625) showing spectrogram of Mirnov magnetic sensor, neutral beam power, and torque (smoothed to strip out modulation effects),  $\beta_N$  and  $D_\alpha$  signals.

- Finally, resonant error fields might be expected to play a role in braking plasma rotation and driving initial tearing mode formation, particularly at low injected torques where a weaker interaction is required to stop rotation.

It is interesting to note that these rotation effects enter in different ways—dependent on absolute rotation, rotation differences between resonant surfaces, local rotation shear, or rotation in a particular frame of reference. Some mechanisms (2, 4, and 5) simply depend on the magnitude of the rotation quantity, others also depend on the sign (1 and 3).

Experiments have already observed indications of some of these mechanisms. For example, studies on the JET (Ref. 27) substituting ion cyclotron resonant heating for neutral beam heating indicated a lowering of the  $\beta$  threshold for the 3/2 NTM.<sup>28</sup> Although the exact mechanism for this dependence was not identified, it is likely that changes in the shielding between the triggering sawtooth event and the NTM resonant surface played a role. Indications that rotation may also be significant for the 2/1 NTM came from error

field studies on DIII-D and JET,<sup>29</sup> which act both to brake plasma rotation and drive formation of magnetic islands on the  $q=2$  surface. On both devices a significant lowering of 2/1 NTM thresholds was found as applied error fields were increased.

The objective of the work described in this paper is to obtain a first full exploration of the rotation effects for the most serious mode, the 2/1 NTM. The study aims to provide both a basic quantification of the effects, and through more detailed analysis and measurement, begin to identify which of the above mechanisms may be playing a role.

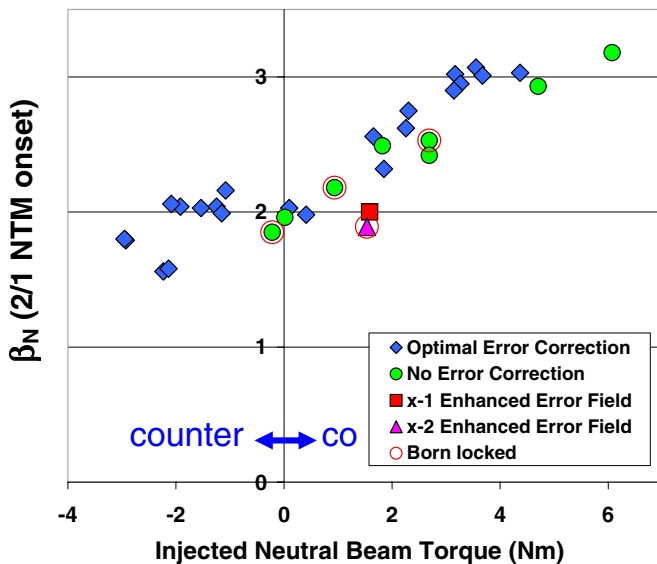
### III. EXPERIMENT CONFIGURATION

Experiments were conducted on DIII-D taking advantage of the fact that one of its four beam lines has been reoriented to inject counter to the usual direction of the plasma current—the other three injecting in the co-direction. Thus, by suitably mixing and modulating the beams, heating power and torque can be controlled independently.

These first rotation studies were performed in sawtoothing ELMy (regimes subject to periodic ELMs) high energy confinement modes of plasma operation (H modes), using a single-null plasma shape with elongation 1.8, triangularity  $\sim 0.53$ , aspect ratio 2.9, similar to that envisaged for ITER baseline operation in order to assess the scale of the effect for the most fundamental ITER regime. Plasma current was 1.03 MA and toroidal field was 1.6 T. The experiments were performed at somewhat increased  $q_{95}$  ( $\sim 4.3$ ) relative to the ITER baseline value of 3.0; this was to provide improved robustness to disruptions and facilitate other secondary studies after mode formation.

Heating power was slowly ramped up to trigger first a 3/2 and then a 2/1 NTM (Fig. 1). The early parts of the discharges were kept as constant as possible between shots (including similar torque values), in order to avoid causing variations in current profile, quality of H mode, etc. In particular, and as a marker for this, in all cases it was ensured that discharges started with clear sawteeth, and that a 3/2 NTM was triggered ahead of the 2/1 NTM. Some time was invested (adjusting density, plasma current, and heating timing) at the start of the study to ensure this could be reliably achieved. The main deviation from this was for net counter-injection discharges, where this recipe was reoptimized to have net counter-beams throughout, as otherwise the pass through zero rotation tended to cause locked modes to form before the counter-phase could be reached.

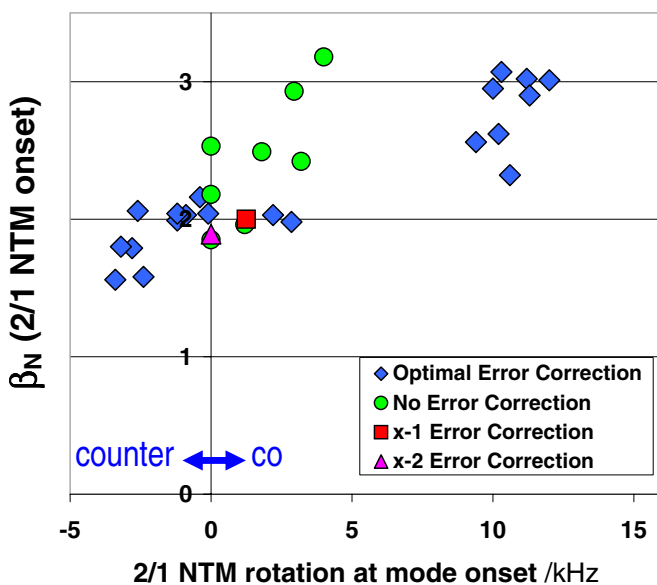
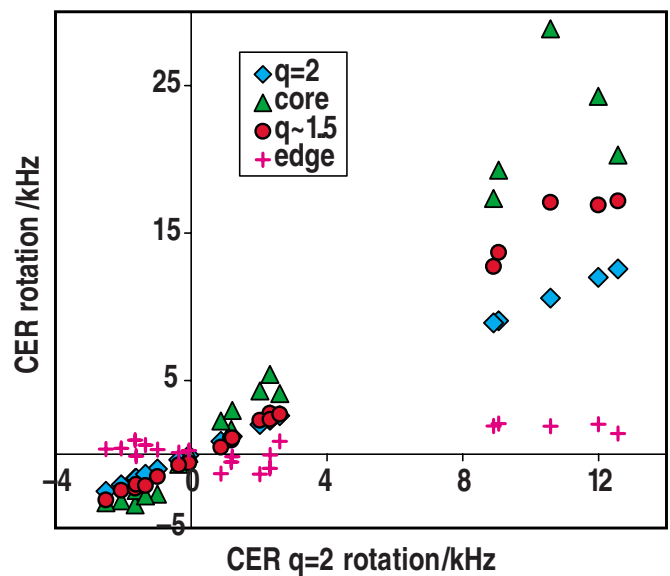
In some discharges, modest levels of error fields were applied using in-vessel “I coils,” or the usual “optimal” error field correction (provided by the I coils) was turned off, to check for possible sensitivities at low rotation to error field modes. (Optimal error field correction is defined as the applied field which operationally gives access to the lowest density in Ohmic density ramp downs. Typically this amounts to around 1.1 Gauss in terms of the 2/1 field harmonic measured at the  $q=2$  surface in straight field line coordinates.)

FIG. 2. (Color online) 2/1 NTM  $\beta_N$  thresholds vs net torque injected.

#### IV. RESULTS: ROTATION DEPENDENCIES

The main results from the experiment are plotted in Fig. 2. This shows a substantial fall in 2/1 NTM onset  $\beta_N$  thresholds from  $\sim 3$  to  $\sim 2$  as the usual strong co-neutral beam torque injection is removed in favor of balanced co-and-counter-beams. The effect is also observed directly when plotted against rotation of the 2/1 mode, although scatter is a little increased, in part due to error fields effects, discussed below.

Interestingly, the removal of the “optimal” error field correction (green circles cf. blue diamonds) appears to have little effect on 2/1 NTM  $\beta_N$  thresholds, suggesting that there is not a greatly increased sensitivity to error fields at low rotation (as might be expected theoretically). Comparing the blue diamonds and green circles in Figs. 2 and 3, we see (somewhat unsurprisingly) that error field appears to be as-

FIG. 3. (Color online) 2/1 NTM  $\beta_N$  thresholds vs initial 2/1 NTM rotation.FIG. 4. (Color online) Comparison of toroidal rotations taken at the core,  $q \sim 1.5$ , and just within the plasma edge with  $q=2$ , using charge exchange spectroscopy.

sociated with a systematic braking of  $q=2$  rotation (being generally displaced to the left of the blue diamonds in Fig. 3). Further reversing and increasing the applied error field (thereby applying an error field of up to 3.4 G of 2/1 field relative to optimal correction—red square and pink triangle) leads only to a modest fall in  $\beta_N$  limits at modest co-injection, comparable with scatter in the data set. In addition, it should be noted that in nearly all cases the NTMs are clearly born rotating, indicating that even at very low levels of torque and plasma rotation, residual error fields are not a strong drive for island formation (which would cause the islands to form locked). These observations provide encouragement that there is not a high error field sensitivity at low rotation, though a full scan of these effects remains a key future issue that should be explored more thoroughly.

Of great theoretical interest is the absence of an upturn in thresholds as net counter-injection and counter-rotation is increased in Figs. 2 and 3. Looking in more detail in Fig. 4 we see that increases in co- or counter-rotation at  $q=2$  are accompanied by corresponding rises of rotation in the core and at  $q \sim 1.5$ . Also the differences in rotation between these various regions also rises with  $q=2$  rotation magnitude. The fact that this happens in the counter-direction (where NTM  $\beta_N$  thresholds do not rise) as well as the co-direction tends to rule out models of NTM seeding in which magnetic coupling to core MHD plays a role, which would lead to rising  $\beta_N$  thresholds with increased rotation differentials in either direction. The data in Fig. 4 also shows that edge rotation (taken  $\sim 2$  cm in from the plasma separatrix, and so in the vicinity of the pedestal top) at the time of NTM onset is generally low, and that differential rotation with respect to  $q=2$  increases with torque in both co- and counter-directions. Thus the lack of increase of NTM  $\beta_N$  thresholds with counter-rotation also tends to suggest that magnetic coupling to edge MHD is not playing a strong role in NTM onset

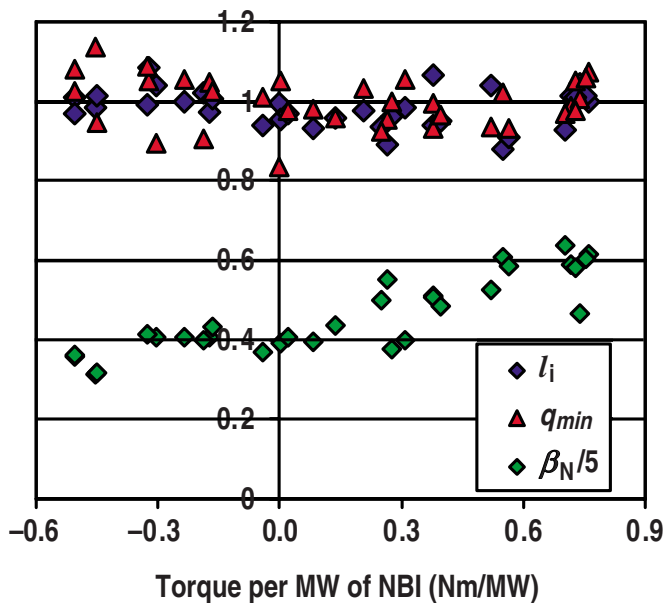


FIG. 5. (Color online) Variation of  $q_{\min}$  and  $l_i$  over the rotation scan, from equilibrium reconstructions constrained by motional Stark effect measurements.

(though ELMs do seem play some role as discussed in the next section). Put simply, the above data indicate that increased rotation and rotation shear magnitudes are not intrinsically stabilizing for the 2/1 NTM, and there does not seem to be a strong role of magnetic coupling to other MHD in the NTM onset. Thus we explore further explanations.

A key point to check before proceeding further is that the switch from co- to counter-beams, which might be expected to deposit differently, did not introduce a change in current profiles, which would affect NTM stability. As discussed in Sec. III, these experiments were optimized to have relaxed sawtooth profiles at the start of heating, so it was hoped that this effect would be negated. To check this, plasma equilibrium reconstructions were carefully optimized using motional Stark effect measurements; resulting measures of profile parameters plasma inductance ( $l_i$ ) and minimum safety factor value ( $q_{\min}$ ) value are plotted in Fig. 5. This indicates no significant systematic difference in current profiles between co- and counter-injected discharges at the time of mode onset.

A key rotation dependency to check is that introduced by the ion polarization current model, which as discussed in Sec. II, can set the threshold for NTM triggering, but depends on the sign and size of propagation of the island  $[\Omega(\text{NTM})]$  in the toroidal frame in which the electric field is zero  $[\Omega(E_{\perp}=0)]$ , relative to ion diamagnetic rotation,  $\omega_i^*$ , at  $q=2$ . This is discussed in Ref. 30, from which the formalism and methods to calculate the appropriate propagation quantity is adopted, based on charge exchange rotation and ion temperature measurements and Thomson scattering electron density and temperatures, including poloidal rotation and diamagnetic contributions. NTM thresholds are plotted against this normalized island propagation frequency in Fig. 6, taking representative points from across the range of the rotation scan. As discussed in Ref. 30 if ion polarization

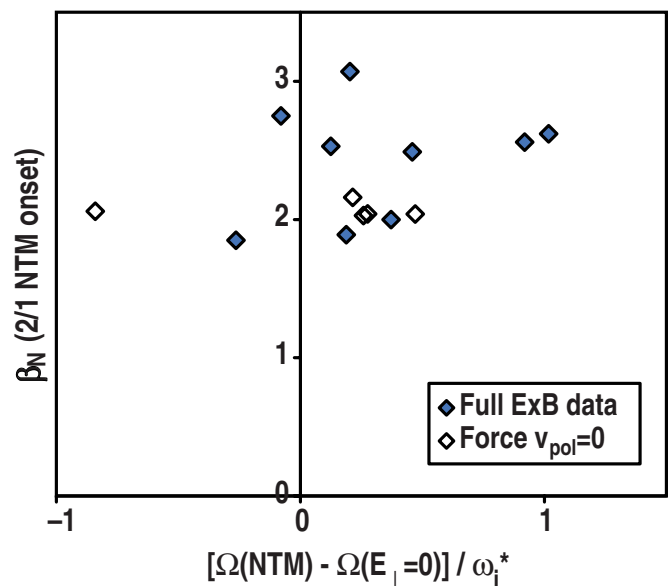


FIG. 6. (Color online) 2/1 NTM thresholds plotted vs island propagation in the toroidal frame in which electric field is zero, normalized to ion diamagnetic rotation (Ref. 29). Open symbols represent additional shots where poloidal rotation was not measured but assumed to be zero (introducing a typical estimated error of 0.05 in  $x$  value).

currents were the only effect governing NTM onset, the plot in Fig. 6 would be expected to have a maximum where its  $x$  axis value is 0.5, and fall substantially as the ion polarization term decreases and then reverses through  $x$  axis values of 0 and 1. Whilst additional physics (e.g., finite island transport effects) would be expected to give some offset to this, a trend should still be discernible if ion polarization effects are playing a significant role. The lack of correlation in Fig. 6, therefore indicates that ion polarization current variations are not responsible for changes in NTM threshold, and are therefore unlikely to be a dominant effect in governing in the onset physics for these 2/1 NTMs. As a further check the analysis was also made replacing  $\Omega(E_{\perp}=0)$  with simple  $q=2$  toroidal rotation (to check that the complex calculation methods and extensive data involved is not introducing excessive noise), but this principally introduced an offset to  $x$  values and still led to no clear trend.

A final point to check in the rotation dependencies is the effect of local rotation shear at  $q=2$ , which can influence NTM thresholds through the  $\Delta'$  term.<sup>25,26</sup> Results for optimal error field correction points, are plotted in Fig. 7, where we have normalized the toroidal rotation gradient ( $d\omega/dR$  in rads/s/m) to the inverse of the magnetic shear scale length,  $L_s = q^2 / [(dq/dr)(r/R)]$  (based on MSE EFITs) and inverse of the Alfvén time,  $\tau_A = R \sqrt{(\mu_0 n_e m_i)} / B_T$ . Whilst there is some scatter in the data, there is a clear and statistically significant trend, with high  $\beta_N$  points at strong net co-rotation and rotation shear, while the points at lowest  $\beta_N$  have some of the most negative rotation shear values. Fit coefficients indicate a coefficient of determination,  $r^2=0.89$  with standard error in  $\beta_N$  of 0.19, while fit parameters have an intercept with zero rotation shear at  $\beta_N=1.98 \pm 0.06$  and a gradient of  $1.90 \pm 0.20$ . The behavior is consistent with models mentioned in Sec. II in which sign and size of rotation shear are

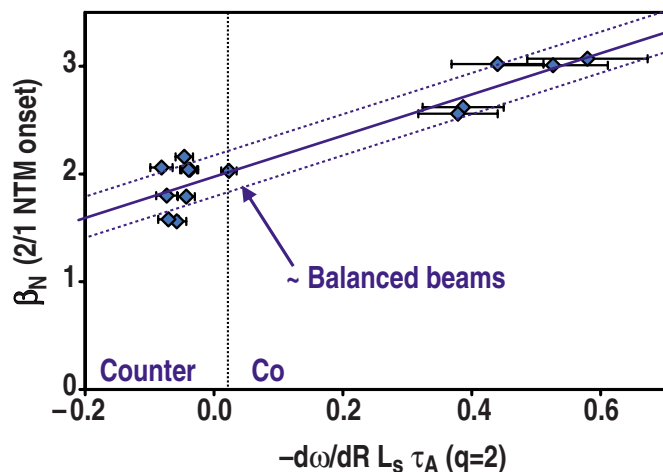


FIG. 7. (Color online) Correlation of 2/1 NTM onset  $\beta_N$  with normalized toroidal rotation gradient (from charge exchange spectroscopy) for optimal error field correction points, as described in the text, with faint lines indicating standard error about fit.

expected to play a role, in terms of whether rotation shear adds to or subtracts from magnetic shear effects in the island. Crucially this is the only model identified that can get this basic trend in the right direction for both co- and counter-data. In order to understand better how this might enter into the NTM  $\beta_N$  threshold dependence, we need to discuss this in the context of the triggering physics, which we do in the next section.

## V. DISCUSSION: HOW ROTATION INFLUENCES 2/1 NTM ONSET

The results in Sec. IV have shown very substantial variations in 2/1 NTM onset  $\beta_N$  thresholds as torque injection to the plasma is varied. However exploration of the variation in various underlying rotation parameters has eliminated many of the most straightforward explanations of behavior, associated with a simple stabilizing role of rotation or differential rotation across the plasma. The data also find little evidence for a rotation effect in the threshold physics via the ion polarization current model. This has left open only one of the possibilities discussed in Sec. II, that local rotation shear may influence thresholds through either raising or lowering  $\Delta'$  values. Here the data indicate considerable scatter, and certainly not a strongly linear or highly correlated effect, but nevertheless, at least an effect that goes in the right direction for both co- and counter-elements of the scan.

To understand how rotation shear may enter into the physics, it is necessary to consider the whole process, including the triggering physics: How is the initial seed island generated? Although these 2/1 NTMs are triggered in sawtoothing baseline scenarios, it is found that the NTM onset almost never occurs near a sawtooth crash. A more probable link to the 2/1 NTM onset comes from the ELMs, which generate magnetic perturbations and send negative pressure waves deep into the plasma (dropping line integrated densities and even core temperatures somewhat). A correlation analysis of the time of onset of the NTM with respect to the ELM is made in Fig. 8. Here shots are categorized according to how

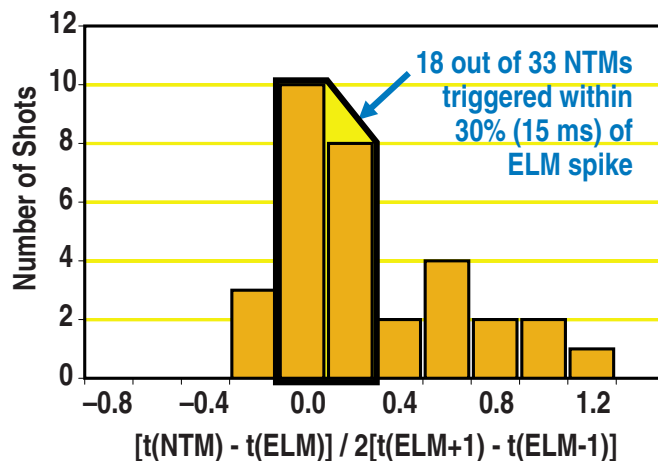


FIG. 8. (Color online) Time correlation between 2/1 NTM onset and large ELMs in DIII-D rotation scan.

close the NTM onset (taken from a magnetics spectrogram) is to the nearest large ELM (taken from  $D_\alpha$  traces, although applying an arbitrary cut in  $D_\alpha$  amplitude at a level associated with the ELM having an observable impact on line average density) normalized to a three-ELM-averaged inter-ELM time for that shot and time. This indicates that the ELM does indeed play a role (as also discussed in Ref. 8), with NTM onset often happening at or soon after a large ELM. However, it is also clear that in about half the discharges there is no such process. Detailed examination of these discharges clearly shows the NTM growing from near zero amplitude, well separated from any evident potential triggering event. Further analysis shows that this mix of “triggered” and triggerless cases occurs across the torque scan—ELM triggering is not associated with a particular beam power or injection direction. Finally, checks also show that the difference between ELM triggered and non-ELM triggered modes does not account significantly for the scatter observed in the NTM  $\beta_N$  thresholds (in Fig. 3).

These observations suggest that in all cases the plasma is close to being intrinsically (e.g.,  $\Delta'$ ) unstable at the point of NTM onset. In some cases the ELM can act to help the process slightly (“the final straw,” perhaps via a pressure wave), but does not have an appreciable effect on  $\beta_N$  thresholds. Thus, having ruled out several other trigger mechanisms, it seems most likely that the 2/1 NTM in these ITER baselinelike ELMy H mode is triggered by the  $\Delta'$  value. A conceptual model can be constructed as a hypothesis to explain the mode onset process, which we will then use to discuss how the various observed dependencies arise:

As  $\beta_N$  is slowly increased towards the ideal  $\beta_N$  limit, the  $\Delta'$  for 2/1 tearing will also increase (i.e., become less negative), even from quite modest values of  $\beta_N$ , well below those where the pole occurs.<sup>5</sup> When  $\Delta'$  becomes positive it will tend to excite small islands. These will grow to some small saturated value,  $w=w_\Delta$  [as indicated by the  $\alpha$  coefficient in Eq. (1) which accounts for saturation effects as discussed in Ref. 18]. These islands will initially be too small to grow neoclassically, as they will fail to flatten bootstrap current due to finite island trans-

port effects [the  $w_d$  term in Eq. (1)]. (But the islands will not be removed by the small island effects as they are not being driven by a hole in the bootstrap current.) However, as the  $\beta_N$  further increases, the “zero island width”  $\Delta'$ ,  $\Delta'_o$ , will rise further and the  $\Delta'$  driven islands will become larger. Eventually they will exceed some critical value,  $w_\Delta > w_{\text{crit}}$  (typically expected to be of the order of double the ion banana width<sup>31</sup>), at which point the pressure gradients in the island will be significantly flattened (overcoming island cross field transport effects), leading to a helical hole in bootstrap current. This will then amplify the island size in the usual way leading to a large saturated NTM.

One can see that this model introduces many of the salient features observed in the NTM physics. The marginal size required for neoclassical growth,  $w_{\text{crit}}$ , will introduce a  $\rho^*$  scaling in the  $\Delta'_o$  required to trigger NTMs, and also in the  $\beta_N$  threshold (as observed in Ref. 8 for the 2/1 NTM). The model also opens the door for rotation shear to affect the NTM threshold by providing an offset to the initial zero island width  $\Delta'$  value,  $\Delta'_o$ . Following the models of Refs. 25 and 26 rotation shear may either give an increase or decrease in  $\Delta'_o$ , and so the  $\beta_N$  rise required to raise  $\Delta'$  and make a large enough island to grow neoclassically will correspondingly be lower or higher.

A key element this model introduces is the prediction of a small “non-neoclassical” island (of width  $w_\Delta$ ) at  $\beta_N$  values below the threshold for large-scale mode destabilization. It would be interesting to search for these experimentally, with refined  $\beta_N$  ramps (going up and down) to distinguish them more clearly from the onset of the large neoclassically driven island. Indeed, some discharges in this experiment exhibited such a phase of protracted weak  $n=1$  mode activity at the 2/1 mode frequency for periods up to 100 ms before growth to large island size ensued. It would be interesting to see whether these “pre-NTMs” decay or freeze in size if the  $\beta_N$  ramp is dropped or frozen slightly after they appear.

With regard to the implications of this model for ITER, the prospects are mixed. The model does point to some negative trends towards larger devices, as critical island widths (normalized to plasma size) required to avoid neoclassical growth fall with  $\rho^*$ , while reduced co-rotation will increase  $\Delta'$ . Both effects would mean smaller  $\beta_N$  rises are required to trigger the 2/1 NTM than in present co-injected, high  $\rho^*$  devices. Given the experimental observations of the clear falls in  $\beta_N$  thresholds with these parameters, any model that did not include such effects would hardly be credible. The positive element comes from the role of the pole in  $\Delta'$  in the model; essentially the mode is triggered as a result of a rise in  $\Delta'$  with  $\beta_N$  as the ideal  $\beta_N$  limit is approached. While the ideal wall beta limit and associated pole in  $\Delta'$  is at high  $\beta_N$  (typically at  $\sim 5-6$ ), the rise in  $\Delta'$  starts at intermediate values of  $\beta_N$ , typically just over half this limit.<sup>5</sup> Thus at lower values of  $\beta_N$ , the variation in  $\Delta'$  with  $\beta_N$  becomes progressively weaker. This suggests that the linear  $\rho^*$  scalings observed in NTM  $\beta$  thresholds in present devices may ease off as we move progressively further from the ideal  $\beta_N$  limit, i.e., there will be a fall to a lower  $\beta_N$  thresholds at lower  $\rho^*$ ,

but perhaps not to the very low levels predicted by a linear extrapolation. This may then open the door to a range of further techniques, such as profile modification (including rotation shear at  $q=2$ , or current profile to affect  $\Delta'$  itself) or localized current drive, to help avoid the mode.

Of course, ultimately ITER may well get these modes, and it should and will be equipped with an electron cyclotron current drive system to help alleviate them. Nevertheless, the best way to treat the problem, if it can be done, is to avoid the modes appearing in the first place. This will reduce requirements on the heating systems and lead to optimum plasma performance.

## VI. CONCLUSIONS

In this paper, we have, for the first time, measured the scaling of the 2/1 NTM  $\beta_N$  limit with plasma rotation for ITER-like sawtoothed ELMy H mode baseline scenarios. Results indicate a fall in this  $\beta_N$  limit from  $\sim 3$  to  $\sim 2$  as co-torque is removed. This raises significant concerns for future devices such as ITER, particularly if it wishes to operate high  $\beta_N$  scenarios with a  $q=2$  surface present. Interestingly, it was also found that as net counter-torque and counter-rotation increase, thresholds do not rise, and if anything, are observed to level out or fall further. This raises additional questions about the physics, which we discuss below. Encouragingly, and on a somewhat a separate line, the low rotation plasmas studied here show no signs of increased susceptibility to error field driven modes, though it might be expected theoretically. These are the main conclusions of this paper. We have also sought to explore the origins of this behavior in terms of the underlying physics concepts, and presented additional results and data that shed light on these questions. Although a quantitative proof of any single model is not demonstrated, we use the observations to identify a possible sequence of processes, consistent with observations and theory made so far. These are summarized below.

The explanation of the rotation dependence in terms of underlying tearing mode physics has been sought. Of particular note is the lack of increase (and even slight decrease) in NTM  $\beta_N$  thresholds with increasing counter-rotation and counter-rotation shear. This tends to suggest magnetic coupling based models (to wall, core MHD, ELMs or error fields) do not play a strong role in governing the 2/1 NTM threshold, and that high magnitude rotation is not “simply” stabilizing for tearing modes. No trend is found in terms of rotation changes related to the ion polarization current model, suggesting it is not dominating the threshold physics. However the sign dependence of the rotation effect does support a model of rotation dependence based on local rotation shear, which may add to or decrease the classical tearing stability index,  $\Delta'$ .

A study of the triggering physics suggests the mode itself is triggered as a result of it being close to intrinsic instability (e.g., through  $\Delta'$ ), although ELMs can and do play a role in the final instability triggering in about half the cases studied. A conceptual model has been outlined as a possible explanation of the process, that may reconcile the dependencies with other observations of  $\rho^*$  scaling of NTM thresh-

olds. This model invokes a  $\beta_N$  related rise in  $\Delta'$ , which would be expected to occur on the approach to a pole associated with the ideal stability limit, to lead to formation of an initial small seed island. This may subsequently grow neoclassically if the  $\Delta'$  driven island reaches large enough size to overcome small island stabilization effects. Local rotation shear (and potentially other profile effects) can effectively offset the  $\Delta'$  value, changing the degree of  $\beta_N$  rise required to make a large enough seed, while  $\rho^*$  dependencies may still arise in the marginal size required for neoclassical growth. These concepts suggest that 2/1 NTM  $\beta_N$  limits might be expected to fall as ITER parameters are approached, but with a progressively weaker dependence as lower  $\rho^*$  values are approached.

These studies indicate that it remains important to plan for electron cyclotron current drive control of 2/1 NTMs in ITER. However further work should be pursued on the NTM physics, first to confirm and extend the above results and physics ideas. Not least, scans need to be extended to more strongly counter-injected discharges, while the effects of error fields near balanced beams needs to be explored in more detail. Secondly, one should also explore how the physics mechanisms discovered here can be exploited to help keep the 2/1 NTM intrinsically stable.

## ACKNOWLEDGMENTS

This work was supported in part by the UK Engineering and Physical Sciences Research Council, by the European Communities under the contract of Association between EURATOM and UKAEA, and by the US Department of Energy under Grant Nos. DE-FC02-04ER54698 and DE-FG02-89ER53297. The views and opinions expressed herein do not necessarily reflect those of the European Commission.

<sup>1</sup>R. J. Buttery, P. Belo, D. P. Brennan, S. Coda, L.-G. Eriksson, B. Gonçalves, J. P. Graves, S. Günter, C. Hegna, T. C. Hender, D. F. Howell, H. R. Koslowski, R. J. La Haye, M. Maraschek, M. L. Mayoral, A. Mück, M. F. F. Nave, O. Sauter, E. Westerhof, C. G. Windsor, the ASDEX Upgrade and DIII-D teams, and JET-EFDA contributors, *Proceedings of the 20th International Conference on Fusion Energy*, Vilamoura, 2004 (IAEA, Vienna, 2004), preprint EX/7-1, <http://www-pub.iaea.org/MTCD/Meetings/PDFplus/fusion-20-preprints/index.htm>.

<sup>2</sup>C. C. Hegna, J. D. Callen, and R. J. La Haye, *Phys. Plasmas* **6**, 130 (1999).

<sup>3</sup>R. J. La Haye, R. J. Buttery, S. Günter, G. T. A. Huysmans, M. E. Maraschek, and H. R. Wilson, *Phys. Plasmas* **7**, 3349 (2000).

<sup>4</sup>D. P. Brennan, E. J. Strait, A. D. Turnbull, M. S. Chu, R. J. La Haye, T. C. Luce, T. S. Taylor, S. Kruger, and A. Pletzer, *Phys. Plasmas* **9**, 2998 (2002).

<sup>5</sup>D. P. Brennan, R. J. La Haye, A. D. Turnbull, M. S. Chu, T. H. Jensen, L. Lao, T. C. Luce, P. A. Politzer, and E. J. Strait, *Phys. Plasmas* **10**, 1643 (2003).

<sup>6</sup>S. Günter, A. Gude, M. Maraschek *et al.*, *Nucl. Fusion* **38**, 1431 (1998).

<sup>7</sup>R. J. Buttery, T. C. Hender, D. F. Howell, R. J. La Haye, O. Sauter, and D. Testa, *Nucl. Fusion* **43**, 69 (2003).

<sup>8</sup>T. C. Hender, D. F. Howell, R. J. Buttery, O. Sauter, F. Sartori, R. J. La Haye, A. W. Hyatt, and C. C. Petty, *Nucl. Fusion* **44**, 788 (2004).

<sup>9</sup>H. R. Wilson, J. W. Connor, R. J. Hastie, and C. C. Hegna, *Phys. Plasmas* **3**, 248 (1996).

<sup>10</sup>R. Fitzpatrick, *Phys. Plasmas* **2**, 825 (1995).

<sup>11</sup>E. Poli, A. G. Peeters, A. Bergmann, S. Günter, and S. D. Pinches, *Phys. Rev. Lett.* **88**, 075001 (2002).

<sup>12</sup>H. R. Wilson, M. Alexander, J. W. Connor *et al.*, *Plasma Phys. Controlled Fusion* **38**, A149 (1996).

<sup>13</sup>R. J. Buttery, S. Günter, G. Giruzzi *et al.*, *Plasma Phys. Controlled Fusion* **42**, B61 (2000).

<sup>14</sup>R. Carrera, R. D. Hazeltine, and M. Kotschenreuther, *Phys. Fluids* **29**, 899 (1986).

<sup>15</sup>O. Sauter, R. J. La Haye, Z. Chang *et al.*, *Phys. Plasmas* **4**, 1654 (1997).

<sup>16</sup>O. Sauter, C. Angioni, and Y. R. Lin-Liu, *Phys. Plasmas* **6**, 2834 (1999); **9**, 5140 (2002).

<sup>17</sup>H. Lütjens, J.-F. Luciani, X. Garbet *et al.*, *Phys. Plasmas* **8**, 4267 (2001).

<sup>18</sup>R. B. White, D. A. Monticello, M. N. Rosenbluth, and B. V. Wadell, *Phys. Fluids* **20**, 800 (1977).

<sup>19</sup>H. Zohm, G. Gantenbein, A. Gude, S. Günter, F. Leuterer, M. Maraschek, J. Meskat, and W. Suttrop, *Phys. Plasmas* **8**, 2009 (2001).

<sup>20</sup>H. Reimerdes, O. Sauter, T. Goodman, and A. Pochelon, *Phys. Rev. Lett.* **88**, 105005 (2002).

<sup>21</sup>M. F. F. Nave, E. Lazzaro, R. Coelho, P. Belo, D. Borba, R. J. Buttery, S. Nowak, and F. Serra, *Nucl. Fusion* **43**, 179 (2003).

<sup>22</sup>M. F. F. Nave, H. R. Koslowski, S. Coda, J. Graves, M. Brix, R. Buttery, C. Challis, C. Giroud, M. Stamp, and P. de Vries, *Phys. Plasmas* **13**, 014503 (2006).

<sup>23</sup>J. P. Graves, C. Angioni, R. V. Budny *et al.*, *Plasma Phys. Controlled Fusion* **47**, 121 (2005).

<sup>24</sup>J. W. Connor, S. C. Cowley, R. J. Hastie, T. C. Hender, A. Hood, and T. J. Martin, *Phys. Fluids* **31**, 577 (1988).

<sup>25</sup>A. Sen, D. Chandra, P. Kaw, M. P. Bora, and S. Kruger, in *Proceedings of the 32nd International Conference on Controlled Fusion and Plasma Physics*, Tarragona, 2005 (European Physical Society, Mulhouse, 2005), Vol. 29C, Preprint P-2.046, <http://eps2005.ciemat.es/papers/html/preface.htm>.

<sup>26</sup>R. Coelho and E. Lazzaro, *Phys. Plasmas* **14**, 012101 (2007).

<sup>27</sup>P. Rebut, R. J. Bickerton, and B. E. Keen, *Nucl. Fusion* **25**, 1011 (1985).

<sup>28</sup>R. J. Buttery, T. C. Hender, D. F. Howell *et al.*, Proceedings of the 28th International Conference on Controlled Fusion and Plasma Physics, Madeira, 2001 (European Physical Society, Mulhouse, 2001), Vol. 25A, p. 1813, <http://www.cfn.ist.utl.pt/EPS2001/fin/index.html>.

<sup>29</sup>R. J. Buttery, R. J. La Haye, T. C. Hender, D. F. Howell, and J. T. Scoville, Proceedings of the 32nd International Conference on Controlled Fusion and Plasma Physics, Tarragona, 2005 (European Physical Society, Mulhouse, 2005), Vol. 29C, pp. 5–60, <http://eps2005.ciemat.es/papers/html/preface.htm>.

<sup>30</sup>R. J. La Haye, C. C. Petty, E. J. Strait, F. L. Waelbroeck, and H. R. Wilson, *Phys. Plasmas* **10**, 3644 (2003).

<sup>31</sup>R. J. La Haye, R. Prater, R. J. Buttery, N. Hayashi, A. Isayama, M. E. Maraschek, L. Urso, and H. Zohm, *Nucl. Fusion* **46**, 451 (2006).